



RAPPORT ANNUEL
2007

Sous projet SC26

Selenium distribution in magmatic sulfide minerals

By

**Richard A. Cox*, L. Paul Bédard*, Sarah-Jane Barnes*,
Marc Constantin****

* Département des Sciences Appliquées, Université du Québec à Chicoutimi (UQAC), Chicoutimi, Québec

** Département de géologie et de génie géologique, Université Laval, Québec, Québec
rcox@uqac.ca

**Soumis à l'administration de DIVEX
juillet, 2007 – Québec**

DIVEX, INRS, Eau Terre Environnement, 490 de la Couronne, Québec, Québec G1K 9A9
Tél. : (418) 654-2652; Fax : (418) 654-2600; Courriel : info@divex.ca; Site web : www.divex.ca

ABSTRACT

The distribution of selenium in the magmatic sulfide minerals has been determined using laser ablation inductively coupled plasma mass spectrometry (LA-ICP-MS). The detection limits and accuracy of Se measurements in sulfide minerals using the LA-ICP-MS are hampered by argide and oxide interferences. The use of a collision cell greatly reduces these interferences and allows for measurement of Se down to a less than a ppm with a spot size of 40 μm . The Merensky Reef (Bushveldt complex, South Africa) and J-M Reef (Stillwater intrusion, Montana, USA) are two of the World's best known magmatic ore deposits. Whole rock data and in-situ LA-ICP-MS measurements, followed by mass balance calculations, suggest that essentially all of the Se in these deposits is contained within the main sulfide phases. This further suggests that micro-extraction of Se from these phases will allow the Se isotopic signature to be used as a tracer for sulfur sources in magmatic sulfide deposits.

1. INTRODUCTION

Selenium (Se) is a chalcophile element generally associated with As, Sb, Te and Bi. There are several rare Se minerals including crookesite ($\text{Cu, Tl, Ag}_2\text{Se}$) and tiemannite HgSe . However, the geochemical distribution of Se is largely controlled by sulfide minerals, such as pyrite, pyrrhotite, chalcopyrite and sphalerite where Se substitutes readily for sulfur (S). Other than magmatic and hydrothermal sulfide deposits, Se is also enriched in red-bed type uranium deposits and diagenetic pyrites. In volcanic systems, Se is volatile and escapes along with other high temperature gasses resulting in low Se-contents for most volcanic rocks. The average Se-abundance in the upper crust is ~ 0.09 ppm (Rudnick and Gao 2004). The average contents of Se in sedimentary rocks are also low, ranging from below 0.05 ppm in clastic sedimentary rocks to 0.08 ppm in marine carbonates (Ebens and Shacklette 1982). However, Se contents are commonly highly elevated in sedimentary rocks which are rich in organic material, such as black shale, where contents can reach ~ 675 ppm (Adriano 1986). In industrial areas, higher than background levels of Se come from the burning of coal, smelting, rubber production and some fertilizers. This has also led to increases of Se in soils and ground waters partly through the adsorption of Se by clay minerals (Kabata-Pendias 2001).

Selenium is highly mobile under oxidizing conditions and in general its mobility decreases with decreasing pH (Gondi et al. 1992). Under reducing conditions Se is immobile. In sub-solidus magmatic systems, Se is

generally less mobile than S and thus, S/Se ratios in whole-rock or mineral samples are sensitive to remobilization of S and to relative S and Se enrichment. For instance, the Se-content and S/Se ratios measured in whole-rock samples has been used as an indicator of magma contamination, sulfide segregation and PGE reef formation in mafic plutonic rocks (e.g. Thériault and Barnes 1998). In most high-temperature geological systems it is assumed that selenium is accounted for by sulfide minerals alone. Such an interpretation is analogous to the behavior of other trace-elements such as the rare-earth elements (REE) which are almost completely controlled by REE-rich phases such as monazite and allanite. This assumption can be readily tested by using mass-balance calculations and whole rock data. This method will also help determine whether the in-situ measurements are accurate. The first aim of this study is to examine the distribution of Se in magmatic sulfide minerals in order to examine the partitioning into the various sulfide minerals present in the well known Merensky and J-M sulfide reefs from the Bushveldt and Stillwater intrusions respectively. Mass balance calculations and whole rock data were also used to help cross-check the results from LA-ICP-MS measurements.

Selenium has six stable isotopes (74, 76, 77, 78, 80, 82). The isotopic composition in geochemical systems can be fractionated by phase transformation (Krouse and Thode 1962, Rees and Thode 1966, Rashid et al. 1978, Rashid and Krouse 1985, Johnson et al. 1999, Herber et al. 2000, Rouxel et al. 2002, Ellis et al. 2003, Johnson and Bullen 2003, 2004, Johnson 2004, Rouxel et al. 2004). The majority of Se-isotopic fraction is controlled by the reduction of Se to lower oxidation states, which in turn is controlled mainly by biological activity (Johnson 2004) and by reduction of soluble oxyanions (Rashid & Krouse 1985, Rouxel et al. 2004). In many respects Se-isotopes behave in a similar manner to the sulfur isotope system, but are much less sensitive to temperature controlled fractionation (Layton-Mathews et al. 2006, Carignan and Wen 2007). Se-isotopes may be used to evaluate country-rock and fluid-magma interactions in magmatic, metamorphic or sedimentary ore-deposits, where the use of the less mobile, less temperature sensitive Se-isotope system could preserve information lost by high temperature re-equilibration of other stable isotope systems. The second aim of this study was to establish a method for Se isotope analysis. However, the experiments are no yet complete. The description presented here is therefore a summary of the progress made so far in determining Se-isotopic compositions.

2. ANALYTICAL METHODS

2.1. Synthesis of Se reference materials and LA-ICP-MS methodology

In order to carry out in-situ trace-element Se determinations, using laser ablation – inductively coupled plasma – mass spectrometry (LA-ICP-MS), a reference material is needed to calibrate the instrument. When possible, it is preferable to have matrix matched reference materials for all in-situ techniques. To this end, we produced a series of synthetic NiS beads doped with Se following a slight modification of the NiS - fire assay bead technique (Robert et al. 1971, Siva-Siddaiah et al. 2000). The beads were made using a known weight of Se standard solution added to the reagents. Powder and solution were then mixed in a clay crucible and heated to 1000 °C in a muffle furnace for 40 minutes. The molten flux was then removed from the furnace and allowed to

cool to room temperature. The exact concentration of selenium in final the NiS bead is difficult to control using gravimetric measurement alone as the sublimated sulfur used in the bead production always contains trace levels of Se. Homogeneous S distribution is expected in the beads, and since Se substitutes directly for sulphur, we expect relatively homogenous Se distribution as well. The major element compositions of each bead were determined using a Cameca SX100 electron microprobe at the University of Laval (Table 1). The results suggest that rapid chilling of the sulfide beads is unnecessary as sulfur distribution is homogeneous.

Since S is homogeneous to within 1.5 % RSD, and assuming that Se substitutes for S in the bead matrix, it was assumed that the bulk Se values determined on these beads would represent valid reference values for subsequent laser ablation analysis. Each bead was split and the Se concentrations were determined by TCF-INAA method of Savard et al. 2006 (Table 1).

Table 1: Concentration of Ni, S and Se in NiS beads. Ni and S determined by electron microprobe at Université Laval and Se by TCF-INAA (Savard et al. 2006).

| Sample # | Ni (wt%) | S (wt%) | Se (µg/g) |
|----------|----------|---------|-----------|
| 122 | 71.55 | 25.83 | 121.9 |
| RSD (%) | 0.12 | 0.62 | |
| 92 | 70.82 | 25.74 | 92.3 |
| RSD (%) | 0.67 | 0.45 | |
| 1120 | 71.62 | 25.46 | 1120 |
| RSD (%) | 0.46 | 1.50 | |

All measurements LA-ICP-MS measurements were made on a Thermo Elemental X7 ICP-MS with a collision cell coupled to a Merchantek New Wave UP-213 laser. Instrumental parameters are presented in Table 2. The laser diameter was 40 µm, with a frequency at 20 Hz and used a power output of 85 % resulting in an energy of 0.112 mJ/pulse. Internal standardisation to correct for ablation yield was done using 34S with the values of sulfur having previously been determined using electron microprobe. The ICP-MS parameters were optimized for low blanks, interferences and maximum sensitivity using the signals generated during ablation of the in-house

reference sulfides. In a typical run the reference sulfides were analyzed twice before and twice after a group of samples, with a maximum of ten unknown samples in each run. All acquisitions were carried out using time resolved signals. Backgrounds and signal areas were selected using the PlasmaLab software (ThermoElemental) which follows the general method of concentration determination as described in Longerich et al. (1996). Signals were selected based on stability and screened for any minute inclusions.

Table 2: Operating conditions for LA-ICP-MS analysis.

| Plasma conditions | |
|--|---|
| RF power (W) | 1250 |
| Plasma gas flow (l min ⁻¹) | 13.02 |
| Auxiliary gas flow (l min ⁻¹) | 0.90 |
| Mass spectrometer settings | |
| Resolution | Standard setting (~1 amu) |
| Isotopes monitored | ³⁴ S, ⁴⁷ Ti, ⁵⁷ Fe, ⁶¹ Ni, ⁶⁵ Cu, ⁶⁶ Zn, ⁷⁴ Se, ⁷⁶ Se, ⁷⁷ Se, ⁷⁸ Se, ⁸⁰ Se, ⁸² Se |
| Dwell time (ms) | 10 |
| Sweeps | 100 |
| Channel per mass | 1 |
| Acquisition duration (ms) | 131 |
| Channel spacing | 0.02 |
| New Wave UP 213 Laser parameters | |
| Wavelength | 213nm |
| Frequency | 20Hz |
| Spot Size | 40 μm |
| Energy | ~0.112 mj/pulse |
| Helium carrier gas flow (l min ⁻¹) | ~0.8 - 1.0 |

It is commonly difficult to obtain accurate Se determinations in sulfide minerals because of a number of major interferences and the low ionization of Se which results in lower than average sensitivity. In particular, strong interferences from argides, argon species created in the plasma, and are especially problematic (Table 3). For example, when attempting to measure the most abundant Se isotope (⁸⁰Se), the most common Ar molecule (⁴⁰Ar⁴⁰Ar) produces a severe interference resulting in backgrounds of several million counts per second.

However, argide interferences on Se can be minimized using a hexapole RF collision/reaction cell in front of the quadrupole mass spectrometer (e.g. Boulyga and Becker 2001). A series of experiments were undertaken to determine the best gas mixture in the reaction cell. A mixture of approximately half of the recommended gas (93 % He + 7 % H₂) and half of a pure H₂ gas gave the best overall interference reduction while maintaining high sensitivity.

Table 3: Summary of major interferences on Se determined by LA-ICP-MS in sulfide minerals.

| Mass of Se | % of Natural Se | Isobaric Interference | % of Isobaric Mass | Oxide Interferences | Argide Interferences |
|------------|-----------------|-----------------------|--------------------|--|--|
| 74 | 0.9 | ^{74}Ge | 36.5 | $^{56}\text{Fe}^{16}\text{O}$ $^{58}\text{Ni}^{16}\text{O}$ | $^{57}\text{Fe}^{17}\text{O}$ $^{56}\text{Fe}^{18}\text{O}$ $^{38}\text{Ar}^{36}\text{Ar}$ $^{36}\text{Ar}^{38}\text{Ar}$ $^{36}\text{S}^{38}\text{Ar}$ $^{34}\text{S}^{40}\text{Ar}$ |
| 76 | 9.0 | ^{76}Ge | 7.8 | $^{60}\text{Ni}^{16}\text{O}$ | $^{59}\text{Co}^{17}\text{O}$ $^{58}\text{Fe}^{18}\text{O}$ $^{58}\text{Ni}^{18}\text{O}$ $^{40}\text{Ar}^{36}\text{Ar}$ $^{38}\text{Ar}^{38}\text{Ar}$ $^{36}\text{Ar}^{40}\text{Ar}$ $^{36}\text{S}^{40}\text{Ar}$ |
| 77 | 7.6 | | | $^{61}\text{Ni}^{16}\text{O}$ | $^{60}\text{Ni}^{17}\text{O}$ $^{59}\text{Co}^{18}\text{O}$ |
| 78 | 23.6 | ^{78}Kr | 0.35 | $^{62}\text{Ni}^{16}\text{O}$ | $^{61}\text{Ni}^{17}\text{O}$ $^{60}\text{Ni}^{18}\text{O}$ $^{40}\text{Ar}^{38}\text{Ar}$ $^{38}\text{Ar}^{40}\text{Ar}$ |
| 80 | 49.7 | ^{80}Kr | 2.25 | $^{64}\text{Ni}^{16}\text{O}$ $^{64}\text{Zn}^{16}\text{O}$ | $^{63}\text{Cu}^{17}\text{O}$ $^{62}\text{Ni}^{18}\text{O}$ $^{40}\text{Ar}^{40}\text{Ar}$ |
| 82 | 9.2 | ^{82}Kr | 11.6 | $^{66}\text{Zn}^{16}\text{O}$ | $^{65}\text{Cu}^{17}\text{O}$ $^{64}\text{Ni}^{18}\text{O}$ $^{64}\text{Zn}^{18}\text{O}$ |

Table 4: Summary of oxide formation based on ablation of pure Ni metal microprobe reference material. The results are shown as ratios of mass 80 (oxide) to metal ratios.

| Reaction gas | Kinetic Energy Barrier | $^{80}\text{NiO}/^{64}\text{Ni}$ | $^{80}\text{ZnO}/^{64}\text{Zn}$ |
|---|------------------------|----------------------------------|----------------------------------|
| None | No | 0.15 | 0.0075 |
| None | Yes | 0.23 | 0.0034 |
| He/H ₂ mix (7% H ₂ in He) | Yes | 0.0088 | 0.000015 |
| He/H ₂ mix plus added H ₂ (50:50) | Yes | 0.0065 | 0.000015 |
| H ₂ only | Yes | 0.00063 | 0.000011 |

Additional interferences on Se caused by oxides formed from Ni, Fe, Co and Zn may also be problematic given the major to minor levels of these elements in most sulfide minerals. However, the dry plasma condition of LA-ICP-MS commonly results in extremely low oxide formation. In order to assess the effects of oxide formation, in particular Ni and Zn oxides, which interfere with the major isotope of Se (^{80}Se) pure Ni and Zn metal microprobe standard were ablated several. The total oxide formation monitored using standard (no collision cell) tuning, standard tuning with the kinetic energy barrier tuning and with the collision cell and various gas mixtures. The results are shown in Table 4.

From shown the results in Table 4, it is clear that with the gas in the collision the oxides are in fact much lower that with conventional tuning. However, there are still minor oxide interferences on ^{80}Se from both Ni and Zn oxides (0.6% - 0.9% and 0.011% - 0.015% respectively). Given the low levels of Zn in the minerals analyzed in this study, correction for Zn oxide is negligible. The correction for Ni oxides was carried out by analysis of a blank NiS bead which was measured several times during each analytical session.

2.2. Results of LA-ICP-MS analysis of Se from natural sulfide samples

The distribution of Se was investigated using the LA-ICP-MS described above. The first set of samples was taken from the upper zone of the Bushveld intrusion in South Africa. This is one of the few localities where Se contents in magmatic sulfide minerals have previously been

determined. Our results (Table 3) compare favorably with proton probe (PIXE) results (Paktunc et al. 1992). In general, the results show that for chalcopyrite and pyrrhotite both LA-ICP-MS and PIXE methods agree well. The apparent difference in Se contents for pentlandite (158 versus 83 $\mu\text{g/g}$) is most likely due to the low number of determinations so far produced (only 2 results reported in Paktunc et al. 1992 and 3 in this study).

Table 5: Se Results by LA-ICP-MS compared with published results on same units.

| | Sulfide | Sample Numbers | Range of Se contents ($\mu\text{g/g}$) | n | Average Se content ($\mu\text{g/g}$) | Uncertainty on Se content ($\mu\text{g/g}$) |
|---------------------|--------------|---------------------------------|--|---|--|---|
| UQAC | Pyrrhotite | 1520.33 | 140-174 | 8 | 160 | 15 |
| Paktunc et al. 1992 | | M1-148.85 M1-52.6 M2-51.5 | 155-206 | 3 | 150 | 5 |
| UQAC | Chalcopyrite | 1520.33 | 116-167 | 7 | 139 | 15 |
| Paktunc et al. 1992 | | M1-148.5 M2-133 M2-51.5 | 141-206 | 3 | 167 | 5 |
| UQAC | Pentlandite | 1520.33 | 156-161 | 3 | 158 | 15 |
| Paktunc et al. 1992 | | M2-51.5 | 63-95 | 2 | 83 | 5 |

A mass balance for Se was calculated using the results in Table 3. The calculation is done assuming that all S is assigned to sulfide, and Se is uniformly distributed in those sulfides. Both are regarded as valid assumptions considering that sulfide minerals are common in these rocks, suggesting S-saturation, and that calculated Se/Se ratios in different sulfide minerals (i.e. $(\text{Se})_{\text{Cpy}}/(\text{Se})_{\text{Po}}$) are approximately one (Paktunc et al 1992). The sample (BV 1520) has a whole rock sulfur content of 1.14 % m/m, Cu of 0.35 % m/m and Ni of 0.1 % m/m (Barnes et al. 2004).

The values are used to estimate the weight proportion (%) of pyrrhotite (po: Fe_{1-x}S), pentlandite (pn: $(\text{Fe}, \text{Ni})_9\text{S}_8$) and chalcopyrite (cp: CuFeS_2) present in rocks. The mass balance for Se is then determined by multiplying the apparent weight proportion of the mineral by the Se concentration:

$$\text{Wt}\%_{\text{cp}} * \text{Se}_{\text{cp}} + \text{Wt}\%_{\text{po}} * \text{Se}_{\text{po}} + \text{Wt}\%_{\text{pn}} * \text{Se}_{\text{pn}} = \text{Se}_{\text{wr}}$$

This gives an estimated whole rock (wr) content of 4.56 $\mu\text{g/g}$ Se which is in agreement with the 4.96 $\mu\text{g/g}$ Se (whole rock value) determined by TCF-INAA (Savard et al. 2006).

From the example above it appear that we can account for

essentially all of the Se in the major sulfide phases. Two further examples were investigate to test this statement, from the Merensky Reef of the Bushveld Complex, and the J-M Reef of the Stillwater Complex. The sample from the Merensky Reef come from the Rustenberg Platinum mine and have between 0.5 to 6 % disseminated sulfides which comprise pyrrhotite, pentlandite and chalcopyrite (Godel et al. 2006). The J-M Reef samples come from the Stillwater mine. Two of the four J-M Reef samples (ST-12 & ST-14) have 2% sulfides while two (ST-16 and 17) have 5 % sulfides (Godel et al. in press). In the Merensky Reef sulfides, Se concentration is higher in pentlandite and pyrrhotite and lowe in chalcopyrite (Table 4) which is in agreement with previous studies of Se contents in sulfides from the Bushveld (Paktunc et al. 1990). There is a slight difference between the results in this study and those reported in Ballhaus and Ryan (1995). However, the samples in Ballhaus and Ryan (1995) were collected from a pothole and those in this study come from a normal reef deposit. The distribution of Se among the sulfides ($\text{Se}_{\text{po}} < \text{Se}_{\text{pn}} < \text{Se}_{\text{Cpy}}$) is in agreement with the order of crystallization and exsolution, i.e.

pentlandite and pyrrhotite exsolving from monosulfide solid solution at ~650 °C, and chalcopyrite exsolving

from intermediate sulfide solid solution at a lower temperatures.

Table 6: In-situ selenium results in Merensky Reef of the Bushveld Complex and the J-M Reef of the Stillwater complex (Bernard 2007).

| Sample | Unit | Pyrrhotite | Pentlandite | Chalcopyrite |
|----------------------|---------------------------|------------|-------------|--------------|
| Merensky Reef | | | | |
| An | Anorthosite | 117 | 176 | 72 |
| CGM-1 | Coarse grained melanorite | 174 | 185 | 150 |
| CGM-2 | Coarse grained melanorite | 152 | 158 | 112 |
| UC + M-1 | Upper chromite | 148 | 187 | 80 |
| M-1 | Melanorite | 155 | 181 | 99 |
| M-2 | Melanorite | 133 | 184 | 105 |
| M-3 | Melanorite | 107 | 113 | 50 |
| M-4 | Melanorite | 143 | 156 | 125 |
| J-M Reef | | | | |
| ST-17 | Olivine melagabbronorite | 247 | 345 | 209 |
| ST-16 | Leuconorite | 219 | 291 | 250 |
| ST-14 | Anorthosite | 231 | 188 | 120 |
| ST-12 | Melatroctolite | 170 | 173 | 371 |

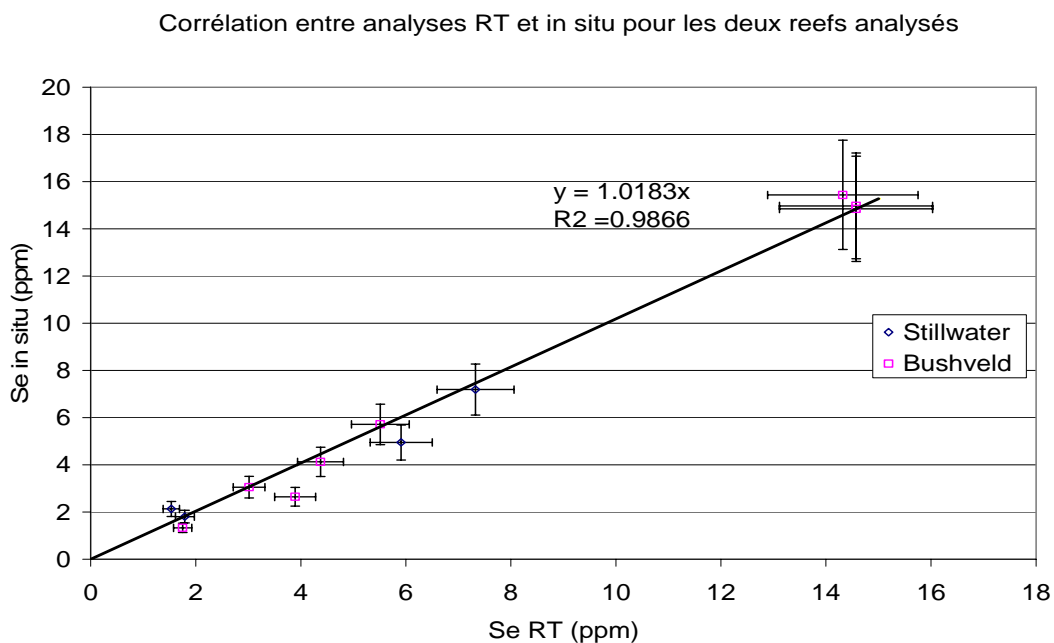
Mass balance calculations were done using whole rocks data from Godel et al. (in press) where all copper is assigned to chalcopyrite and nickel to pentlandite. The mass fractions for the sulfides are presented in Table 6. According to Godel et al. (in press) there is 44% Pn, 37% Po and 19 Cpy in the Merensky Reef and 33% Pn, 46 % Po and 21% Cpy in the J-M Reef. Results for these mass balance calculations are presented in Figure 1. In general the results suggest that the Se contents determined by LA-ICP-MS *in-situ* agree with whole rock results. This supports the conclusion above that essentially all the Se is contained within the major sulfides. Any slight

discrepancies are generally within analytical errors. However, it may also be possible that Se is also contained within minor and accessory phases not intercepted during ablation. This would also explain the slight differences between the two data sets. We are currently carrying out a series of X-ray maps which will attempt to locate and characterize any Se-bearing phases that were missed during the initial LA-ICP-MS analyses.

Table 7: Mass fraction of the sulfides.

| Sample | FCp | Fpn | Fpo |
|----------------------|-------------|-------------|-------------|
| Merensky Reef | | | |
| An | 0.002648617 | 0.003728133 | 0.00405116 |
| CGM-1 | 0.010248902 | 0.039721043 | 0.037453665 |
| CGM-2 | 0.012706856 | 0.014412054 | 0.013147874 |
| UC + M-1 | 0.004160475 | 0.007296954 | 0.003962264 |
| M-1 | 0.008308605 | 0.043868076 | 0.039898953 |
| M-2 | 0.00296824 | 0.008961681 | 0.009406418 |
| M-3 | 0.003241014 | 0.01218425 | 0.010247758 |
| M-4 | 0.004140787 | 0.012481426 | 0.011550246 |
| J-M Reef | | | |
| ST 12 | 0.0062 | 0.0083 | 0.007 |
| ST 14 | 0.0018 | 0.0025 | 0.0048 |
| ST 16 | 0.0052 | 0.0101 | 0.0134 |
| ST 17 | 0.0014 | 0.0023 | 0.0042 |

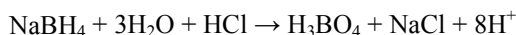
Fig. 1: In-situ Se against Se in whole rock (RT) for Merensky and J-M Reef from Bernard 2007.



2.3. Selenium isotope determinations: general methodology and current status

The initial aim of this study was to determine whether the Se isotope compositions could be used as an indicator of sulfur source (magmatic, contamination, etc.) and thus, elucidate the formation of magmatic sulfide deposits. In order to determine with any degree of accuracy the Se isotope composition of a sample a number of procedures are required. Firstly, the Se has to be separated from its matrix. This involves the digestion of the sample at low temperatures to avoid loss or fractionation of Se due to volatility. Secondly, Se is concentrated and the other matrix elements removed using a thiol cotton fiber (TCF) exchange column (e.g. Savard et al. 2006). Once the Se is trapped on the column, the matrix elements are washed out, and the Se recovered by desorption of the TCF (Rouxel et al. 2002, 2004). The Se concentrate solution can then be introduced to the ICP-MS for measurement of the isotopic ratios. However, there are two major problems with ICP-MS analysis of Se. Selenium has a low ionization potential in ionic form. This means that during analysis much lower number of ions are formed in the plasma resulting in poor signals. This can be overcome by converting Se to its hydride form. The general reactions for forming a Se-hydride are:

1 - (Reaction forming hydrogen):



2 - (Sample/hydride formation to ICP-MS):



The hydride formation has to be controlled using a series of solutions, a pump, mixing and reaction coils and a gas-liquid separator, which are collectively called a hydride generator. Three hydride generation systems have been tested so far, a ICAP 6000 HG accessory (Thermo Instruments), a VGA-77 Automatic Vapor Generator (Varian Inc.) and a custom made systems similar to those described in Rouxel et al. (2002) and Layton-Matthews (2006). The main problem with the former systems is that the small mixing and reaction chambers employed by these systems do not allow for a high throughput of Se-solution and reagents (typically less than 0.5 ml/min). The result is that the total Se counts are low and thus, the overall precision of isotopic ratios is not sufficiently precise for geologic problems. The custom made system allowed for much higher sample throughput (>1 ml/min) resulting in significantly better signals and therefore improved isotopic ratio precision. The second major obstacle to be overcome in ICP-MS measurement of Se isotopes is the presence of argide interferences as

described above. However, building on our experience with LA-ICP-MS measurements we have been able to use the collision cell to essentially eliminate this problem. Unfortunately, we have not had time to fully test our customized hydride system and our initial results are limited to around 1% precision. In addition, we have only just received the latest NIST Se-isotope reference material (Carignan and Wen 2007). We are therefore continuing to develop the method and will shortly begin testing the improved hydride generator with natural samples and the NIST reference material.

3. CONCLUSIONS

The measurement of Se contents and subsequent mass balance calculations presented in this study show that the Se budget is controlled by the main sulfide minerals within magmatic ore bodies. Subsequent studies will involve detailed X-ray mapping and LA-ICP-MS grid analyses of these phases in order to show conclusively that Se is indeed hosted within the crystal structure and not incorporated into accessory phases. The methodology for measuring Se isotopes is currently under development. One encouraging result of the LA-ICP-MS analyses in this study is that the majority of Se is indeed contained within the main sulfide ore minerals. Thus, it will be relatively easy to extract Se from these phases. This will allow highly pure and enriched concentrates of Se to be prepared for subsequent isotopic analysis, the results of which will be directly interpretable in terms of the formation mechanisms of the ore bodies themselves.

4. References

- Adriano, D.C., 1986. Trace elements in the terrestrial environment. Springer, New York.
- Ballhaus, C. and Ryan, C., G., 1995. Platinum-group elements in the Merensky Reef. I. PGE in solid solution in base metal sulfides and the down-temperature equilibration history of Merensky ores. *Contributions to mineral petrology*, 122: 241-251.
- Barnes, S.-J., Maier, W.D., Ashwal, L. D. 2004. *Chemical Geology, Platinum-group element distribution in the Main Zone and in the Upper Zone of the Northern Limb of the Bushveld Complex*. 208: 293-317.
- Bédard, L.P., Bernard, J., Barnes, S.-J. 2007. Searching for selenium: in situ measurement in base metal sulfides. *Goldschmidt conference abstract*.
- Bernard, J. 2007. Analyse du sélénium roche totale et dans les sulfures du Merensky Reef (Complexe du Bushveld, Afrique du Sud) et du J-M Reef (Complexe du Stillwater, Montana, USA). Rapport de stage,

Université du Québec à Chicoutimi, 36 pp.

Ebens, R.J. and Shacklette, H.T., 1982. Geochemistry of some rocks, stream sediments, soils, plants, and waters in the western energy region of the conterminous United States. U.S. Geological Survey

Prof. Paper 1237. U.S. Government Printing Office, Washington D.C., 173 pp.

Carignan, J. Wen, H. 2007. Scaling NIST SRM 3149 for Se isotopes analysis and isotopic variations of natural samples. *Chemical Geology*, 242, 347-350.

Ellis, A.S., Johnson, T.M., Bullen, T.D., Herbel, M.J., 2003. Stable isotope fractionation of selenium by natural microbial consortia. *Chemical Geology* 195, 119–129.

Godel, B. Barnes, S.-J., Maier, W. 2006. 3-D distribution of sulfide minerals in the Merensky Reef (Bushveld Complex, South Africa) and the J-M Reef (Stillwater Complex, USA) and their relationship to microstructures using X-ray computed tomography. *Journal of Petrology*, 47: 1853-1872.

Godel, B. Barnes, S.-J., Maier, W. In Press. Platinum-group elements in sulphide mineral, platinum-group metals, and the whole rock of the Merensky Reef (Bushveld Complex, South Africa): Implication for the formation of the Reef. *Journal of Petrology*

Godel, B. Barnes, S.-J., Maier, W. In Press. Platinum-group elements in sulphide mineral and the whole rock of the J-M Reef (Stillwater Complex): Implication for the formation of the Reef. *Chemical Geology*.

Gondi, F., Panto, G., Feher, J., Bogy, G. Alftan, G. 1992. Selenium in Hungary: The rock-soil-human systems. *Biological Trace-Element Research*, 35, 299-306.

Herbel, M.J., Johnson, T.M., Oremland, R.S., Bullen, T.D., 2000. Selenium stable isotope fractionation during bacterial respiratory reduction of selenium oxyanions. *Geochimica Cosmochimica Acta* 64, 3701–3709.

Johnson, T.M., Bullen, T.D., 2003. Selenium isotope fractionation during reduction of Fe(II)–Fe(III) hydroxide–sulfate (greenrust). *Geochimica Cosmochimica Acta* 67, 413–419.

Johnson, T.M., Bullen, T.D., 2004. Mass-dependent fractionation of selenium and chromium isotopes in low-temperature environments. In: Johnson, C.M., Beard, B.L., Albarède, F. (Eds.), *Geochemistry of non-traditional stable isotopes*, *Reviews in Mineralogy and Geochemistry*, vol.55. Mineralogical Society of America–Geochemical Society, Washington D.C., USA, pp. 289-317.

Johnson, T.M., Herbel, M.J., Bullen, T.D., Zawislansky,

P.T., 1999. Selenium isotope ratios as indicators of selenium sources and oxianion reduction. *Geochimica & Cosmochimica Acta* 63, 2775–2783.

Kabata-Pendias, A., 2001. Trace elements in soils and plants (3rd edition). CRC press, Boca Raton, Florida.

Krouse, H.R., Thode, H.C., 1962. Thermodynamic properties and geochemistry of isotopic compounds of selenium. *Canadian Journal of Chemistry* 40, 367–375.

Layton-Matthews, D., Leybourne, M., Peter, J.M., Scott, S.D., 2006. Determination of selenium isotopic ratios by continuous-hydride-generation dynamic-reaction-cell inductively coupled plasma-mass spectrometry. *Journal of Analytical Atomic Spectrometry*, 21, 41-49.

Longerich, H. P. , Jackson, S. E., Günther, D., 1996. Laser ablation inductively coupled mass spectrometry transient signal data acquisition and analyte concentration calculation. *Journal of Analytical Atomic Spectrometry*, 11, 899.

Rees, C.B., Thode, H.G., 1966. Selenium isotope effects in the reduction of sodium selenite and of sodium selenate. *Canadian Journal of Chemistry* 44, 419–427.

Rashid, K., Krouse, H.R., 1985. Selenium isotopic fractionation during SeO₃ reduction to Se⁰ and H₂Se. *Canadian Journal of Chemistry* 63, 3195–3199.

Rashid, K., Krouse, H.R., McCready, R.G.L., 1978. Selenium isotope fractionation during bacterial selenite reduction. In: Zartman, R.E. (Ed.), *Short papers of the Fourth International Conference, Geochronology, Cosmochronology, Isotope Geology*. Open-File Report-U.S. Geological Survey, Reston, VA, United States, pp. 347–348.

Robert, R.D., van Wyk, E., Palmer, R., 1971. Concentration of the noble metals by a fire assay technique using nickel-sulphide as the collector. National Institute of Metallurgy, South Africa, report 1371, 1-16.

Rouxel, O., Ludden, J.N., Carignan, J., Marin, L., Fouquet, Y., 2002. Natural variations of Se isotopic composition determined by hydride generation multiple collector inductively coupled plasma mass spectrometry. *Geochimica & Cosmochimica Acta* 66, 3191–3199.

Rouxel, O., Fouquet, Y., Ludden, J.N., 2004. Subsurface processes at the Lucky Strike hydrothermal field, mid-Atlantic ridge: evidence from sulfure, selenium and iron isotopes. *Geochimica & Cosmochimica Acta* 68, 2295–2311.

Rudnick, R.L. & Gao, S., 2004. Composition of the

continental crust. In: Treatise on Geochemistry (Vol. 3): The Crust. (ed. R.L. Rudnick). Elsevier, Amsterdam, pp1-64.

Savard, D., Bédard, L.P., Barnes, S.-J., 2006. TCF selenium preconcentration in geological materials for determination at sub- $\mu\text{g g}^{-1}$ with INAA (Se/TCF-INAA). *Talanta*, 70, 566-571.

Siva Siddaiah, N., Masuda, A., Hirata, T. 2000. Geoanalysis 2000 program with abstracts, CRPG, Vandoeuvre-lès-Nancy, France, p. 113.